A numerical study of projectile impact on mild steel armour plates

M. Raguraman[1], A. Deb[1,*] and N. K. Gupta[2]

[1]Centre for Product Design and Manufacturing, Indian Institute of Science, Bangalore 560 012, India
[2]Department of Applied Mechanics, Indian Institute of Technology Delhi, Hauz Khas, New Delhi 110 016, India

The present article deals with the development of a finite element modelling approach for the prediction of residual velocities of hard core ogival-nose projectiles following normal impact on mild steel target plates causing perforation. The impact velocities for the cases analysed are in the range 818–866.3 m/s. Assessment of finite element modelling and analysis includes a comprehensive mesh convergence study using shell elements for representing target plates and solid elements for jacketed projectiles with a copper sheath and a rigid core. Dynamic analyses were carried out with the explicit contact-impact LS-DYNA 970 solver. It has been shown that proper choice of element size and strain rate-based material modelling of target plate are crucial for obtaining test-based residual velocity. The present modelling procedure also leads to realistic representation of target plate failure and projectile sheath erosion during perforation, and confirms earlier observations that thermal effects are not significant for impact problems within the ordnance range. To the best of our knowledge, any aspect of projectile failure or degradation obtained in simulation has not been reported earlier in the literature. The validated simulation approach was applied to compute the ballistic limits and to study the effects of plate thickness and projectile diameter on residual velocity, and trends consistent with experimental data for similar situations were obtained.

Keywords: Ballistic impact, finite element modelling, mild steel plate, projectile.

NONLINEAR finite element-based contact–impact analysis is a versatile tool for predicting projectile residual velocities and ballistic limits for impact on armour plates. The primary objective of the numerical studies reported by different investigators has been to show that the analysis results can correlate against experimental results, including failure. Most of the finite element modelling procedures discussed in the open literature employ plane strain or axisymmetric finite element representation[1–3] of projectiles and target plates. However, a limitation of this approach, with consideration given only to mechanics and less attention paid to requirements of design, lies in its inability to simulate oblique impact of projectiles, targets of arbitrary shapes, off-centred impact, etc. In the present study, plates were represented with shell elements and projectiles with solid elements. This constitutes a general modelling approach in which three-dimensional and non-axisymmetric behaviours can be captured. For constitutive modelling of target plates, published data on strain rate dependence of yield and failure strengths of steel alloys have been used to generate true stress vs true strain curves of relevant mild steel target plates at discrete strain rates. The specification of yield stress and ultimate strength for a number of strain rates along with a tangent modulus is equivalent to providing a set of parallel effective flow stress vs effective plastic strain (up to failure) curves at a given strain rate. This approach allows modelling of expected reduction in uniaxial failure strain of a ductile material with increasing strain rate. It may be noted that the present elasto-plastic material modelling procedure essentially involves a rate-dependent Von Mises yield criterion combined with isotropic strain hardening; this is an extension of the commonly used approach for analysing nonlinear material behaviour of ductile materials for quasi-static loading and may appeal to design engineers. The effects of adiabatic heating that can potentially lead to localized phase transformation in the interacting components, i.e. projectile and target, have not been accounted for here. This approach is consistent with earlier observations[4] that the medium range of impact velocities (in the ordnance range) considered in the present study is unlikely to induce thermal changes in steel that will perceptibly change its material behaviour.

While material behaviour under dynamic conditions as explained above is a key consideration in analysing the mechanics of projectile and target interaction, other parameters such as mesh density and contact algorithm can significantly affect simulation results. In order to establish the required modelling criterion in terms of element size, a detailed convergence study of residual velocity has been carried out for thin to moderately thick plates by varying mesh density in the impact zone. The residual velocities computed using explicit LS-DYNA solver were compared against test results presented in Gupta and Madhu[5] for normal impact on three variants of mild steel target plates with ogival-nose jacketed projectiles and excellent correlation was obtained. The impact velocities for the problems

*For correspondence. (e-mail: adeb@cpdm.iisc.ernet.in)

solved lay in the range 818–866.3 m/s. Details of simulation-based plate failure and projectile sheath erosion have been presented and appear to be consistent with the experimentally observed phenomena in Gupta and Madhu[5]. The consequences of ignoring strain rate effect in target constitutive model have been shown. Finally, using the validated modelling procedure, the effect of design parameters such as plate thickness and projectile diameter on residual velocity of the projectile was studied and physically consistent trends obtained.

Finite element modelling of projectile and target plate

A finite element model of a given target plate using shell elements and a projectile represented with solid elements is shown in Figure 1. For analysis using LS-DYNA, Belytschko–Lin–Tsay shell elements were chosen. The incremental explicit dynamic analysis was based on a co-rotational formulation for shells. A detailed view of the jacketed ogival-nose projectile is given in Figure 2. To start with, these models were employed for studying the effect of plate finite element mesh size on convergence of computed projectile residual velocity with respect to test values given in Gupta and Madhu[5]. The plate was square in shape with dimensions of 200 mm × 200 mm, and was clamped at its four corners. Plates of five different thicknesses, viz. 4.7, 6, 10, 12 and 16 mm were considered. These plates were made of three variants of mild steel (MS) as given in Gupta and Madhu[5]. The projectile core had a diameter of 6.2 mm, was 28 mm long and weighed 5.2 g. It was made of a hard steel alloy with an approximate hardness of 900 VPN. The core was enclosed in a copper sheath, which increased the total diameter of the shot to 7.8 mm.

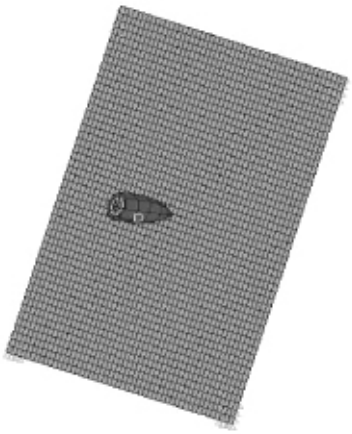

Figure 1. Plate modelled with shell elements being impacted centrally with a jacketed projectile.

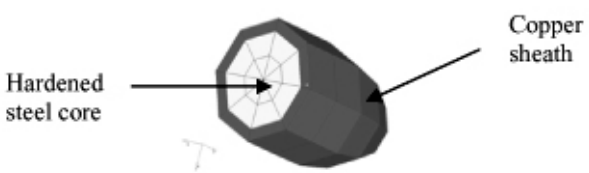

Figure 2. Modelling of jacketed projectile with solid elements.

Material modelling

The material model with the keyword *MAT_STRAIN_RATE_DEPENDENT_PLASTICITY (material type 19) in LS-DYNA was used for defining the behaviours of three variants of MS plates designated as MS1, MS2 and MS3 in Gupta and Madhu[5]. In this constitutive model, yield and tensile strength can be specified in a tabular manner with respect to strain rate. The quasi-static engineering properties of these steel plates for the hardness ranges quoted in Gupta and Madhu[5] are given in Table 1.

The quasi-static engineering properties were at first converted to corresponding true values. Conversion of engineering to true stress was carried out using the relation given below (assuming constant volume of a uniaxial test specimen):

$$\sigma^{\text{true}} = (\varepsilon^{\text{eng}} + 1)\sigma^{\text{eng}}, \tag{1}$$

where σ^{true} is the true stress, while ε^{eng} and σ^{eng} are the engineering (i.e. nominal) strain and corresponding engineering (i.e. nominal) stress respectively.

True logarithmic strain, $\varepsilon^{\text{true}}$ was obtained from the following relation:

$$\varepsilon^{\text{true}} = \ln\left(\frac{l}{l_0}\right) = \ln(\varepsilon^{\text{eng}} + 1), \tag{2}$$

where l and l_0 are the instantaneous and initial gage lengths of a uniaxial test specimen respectively.

The true failure strain, $\varepsilon_{\text{f}}^{\text{true}}$ was estimated by substituting the value of uniaxial engineering failure strain in the right hand side of eq. (2) for a given MS plate from Table 1. The true yield strain, $\varepsilon_{\text{y}}^{\text{true}}$ and tangent modulus, E_{T} were computed as follows:

$$\varepsilon_{\text{y}}^{\text{true}} = \frac{\sigma_{\text{y}}^{\text{true}}}{E}, \tag{3}$$

$$E_{\text{T}} = \frac{\sigma_{\text{f}}^{\text{true}} - \sigma_{\text{y}}^{\text{true}}}{\varepsilon_{\text{f}}^{\text{true}} - \varepsilon_{\text{y}}^{\text{true}}}. \tag{4}$$

Using eqs (1)–(4), the relevant quasi-static true material parameters have been computed for variants of steel plate targets (assuming a standard value of E = 205 GPa for all cases) and are listed in Table 2.

Table 1. Quasi-static engineering properties of MS plates

Plate material nomenclature in Gupta and Madhu[5]	Vickers hardness range in Gupta and Madhu[5]	Quasi-static yield strength (MPa)	Quasi-static tensile strength (MPa)	Quasi-static elongation at break (%)
MS1	110–115	205	380	25
MS2	150–155	360	505	35
MS3	140–145	305	465	34

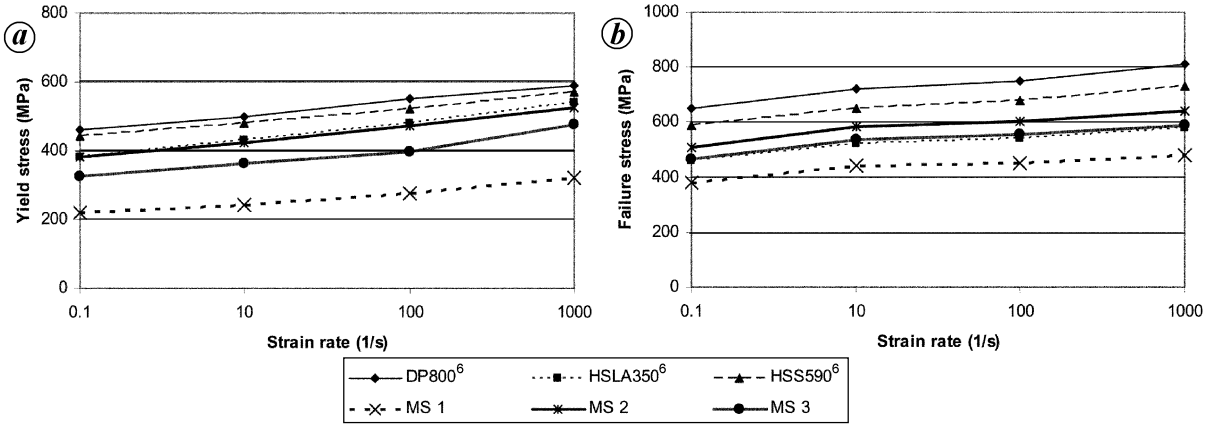

Figure 3. Stresses of variants of steel with respect to strain rate: ***a***, Yield; ***b***, Ultimate.

Table 2. True quasi-static properties of MS1, MS2 and MS3

Plate material	σ_y^{true} (MPa)	σ_f^{true} (MPa)	ε_y^{true} (%)	ε_f^{true} (%)	E_T (MPa)
MS1	205.4	475	0.100	22.0	1233
MS2	360.0	682	0.176	30.0	1079
MS3	305.0	623	0.149	29.3	1092

Variations of yield and tensile strength with respect to strain rate for three varieties of steel designated as DP800, HSLA350 and HSS590 have been reproduced from Benda[6] in Figure 3 *a* and *b*. It can be observed from Figure 3 that the rise in yield and failure stresses with respect to strain rate is more or less independent of the type of steel considered in Benda[6]. Hence similar variations of yield and failure stresses with reference to strain rate are adopted for the present mild steel variants (MS1, MS2 and MS3) of target plates as shown in Figure 3 *a* and *b* respectively. In particular, the following scaling relation was applied to obtain the dynamic yield and failure strengths of mild steel plates considered here:

$$\sigma_{\dot{\varepsilon}}^{(\text{steel type})} = \sigma_{\dot{\varepsilon}_0}^{(\text{steel type})} \cdot \frac{\sigma_{\dot{\varepsilon}}^{(\text{HSS590})}}{\sigma_{\dot{\varepsilon}_0}^{(\text{HSS590})}}, \tag{5}$$

where $\sigma_{\dot{\varepsilon}}^{(\text{steel type})}$ is the strength (yield or failure) at a given strain rate, $\dot{\varepsilon}$ (s^{-1}), and $\sigma_{\dot{\varepsilon}_0}^{(\text{steel type})}$ is the corresponding quasi-static strength at a low strain rate of $\dot{\varepsilon}_0$ (s^{-1}). A regression-based curve-fitting approach has been used to obtain the yield and failure strengths of a target material by extrapolation at a high strain rate (e.g. 10,000 s^{-1}) not considered in Benda[6].

The approach outlined above leads to a set of true stress–strain curves for various strain rates for each mild steel variety being studied here for projectile impact. These bilinear strain rate-dependent elastic–plastic material behaviours are given in Figure 4 *a–c* respectively for MS1, MS2 and MS3. It may be noted that it is common practice to employ bilinear elastic–plastic stress–strain variations[7–11] for metals in analytical and numerical procedures. This yielded acceptable predictions, especially when energy-based criteria are involved in governing failure. This bilinear elastic–plastic behaviour has been referred to as Illyushin's model in the literature[11]. The basic idea here has been that the total area under a bilinear approximation of stress–strain variation was adjusted to match the area under the exact stress–strain curve obtained in a uniaxial test. The yield stress in the bilinear assumption was generally close to the lower yield point for mild steel.

The projectile core has been assumed as rigid based on the physical observation that only sheath erosion occurred in the tests carried out in Gupta and Madhu[5], against which comparisons have been made here. The sheath is modelled with material type 24 in LS-DYNA, designated with the keyword *MAT_PIECEWISE_LINEAR_PLASTICITY, using the nominal engineering properties

of copper listed in Table 3. It may be noted that strain rate sensitivity has not been considered in the material modelling of projectile. In the target plate material model, the viscoplastic formulation option was chosen for analysis.

Effect of element size on projectile residual velocity

The objective of this study was to determine an optimal shell element size for the target plate which will yield reliable values of projectile residual velocity. Plates of thickness in the range of 4.7–16 mm and material grades as specified in Gupta and Madhu[5] were considered. The computed residual velocities have been compared in Figure 5 *a–e* with the corresponding measured values reported in Gupta and Madhu[5]. For plates up to a thickness of 10 mm, excellent convergence of computed residual velocity to test residual velocity was observed, while for 12 and 16 mm thick plates, the computed residual velocities were lower than the corresponding test residual velocities, perhaps due to under prediction of transverse shear deformation in a shell element formulation. In general, however, extremely good monotonic convergence was seen for all cases in Figure 5. The contact algorithm in LS-DYNA chosen for analysis was surface-to-surface with erosion. Coefficients of static and dynamic friction were assigned values of 0.2 and 0.1 respectively, as is common practice. It may be concluded from this study that shell elements of size 1–1.5 mm may be used for simulating impact on MS target plates of aspect ratio (thickness/length) 0.02–0.08.

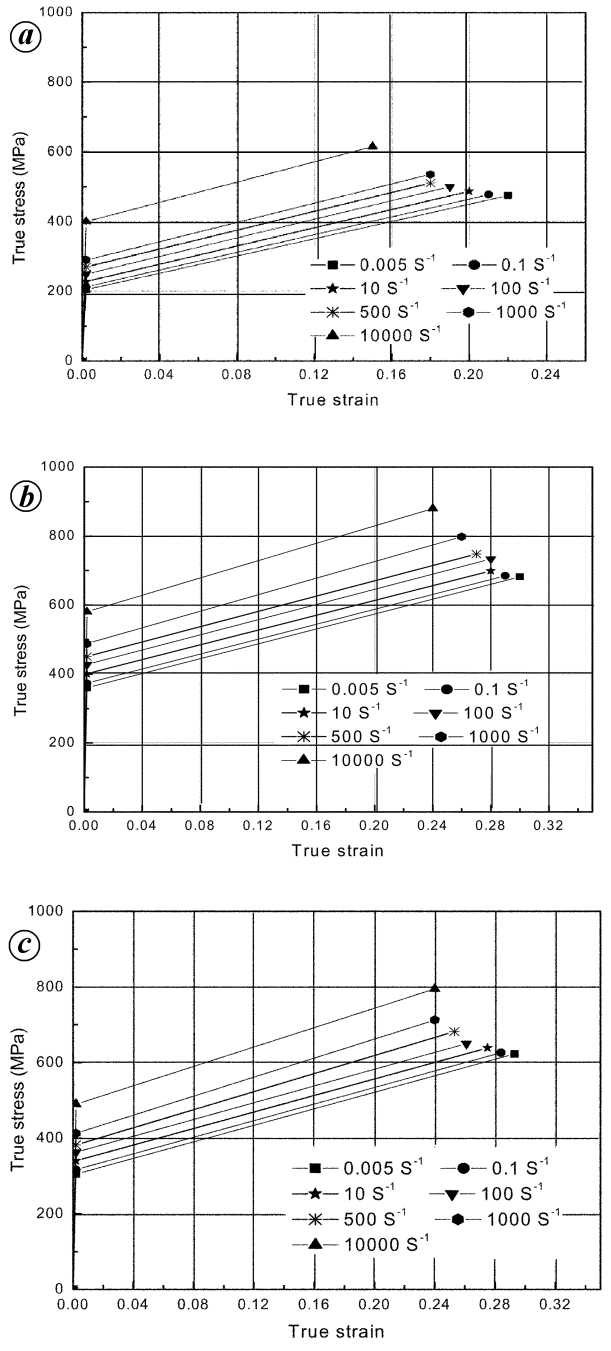

Figure 4. True stress versus true strain behaviour of plates MS1–MS3. ***a***, MS1; ***b***, MS2; ***c***, MS3.

Effect of shell element type on residual velocity

The Belytschko–Lin–Tsay shell element based on a corotational formulation was chosen for the preceding analysis, as it is computationally efficient and is the default shell element in LS-DYNA. Alternatively, Hughes–Liu shell elements could be used for analysing the present impact problems. However, for a shell element with five through-the-thickness integration points, the Belytschko–Lin–Tsay shell element requires 725 mathematical operations compared to 4066 operations for the under-integrated Hughes–Liu element[12]. In addition to their computational efficiency, the Belytschko–Lin–Tsay shell elements, for the same mesh density, have been found by the present authors to yield comparable values of residual velocity as the Hughes–Liu shell elements (Table 4).

Effect of mesh configuration on residual velocity

It has been shown that discretization of plate mid-surface with square shell elements of appropriate size leads to converged residual velocities that correlate well with test results. The perforations created in such meshes are also square-shaped, as shown in Figure 6 for a 16-mm thick MS3 plate analysed earlier. Perforations in actual plate impact tests due to normally impinging cylindrical bullets of various nose shapes were essentially of circular periphery, as indicated in the published literature. Such nearly circular holes as in Figure 7 *b*, primarily due to shear plugging, can be obtained through analysis if triangular shell elements with a disposition of circular symmetry as illustrated in Figure 7 *b* are used for meshing the target plate. The shape of the perforation is thus controlled by the configuration

Table 3. Projectile properties used in simulation

Projectile component	Elastic modulus (GPa)	Poisson's ratio	Yield strength (MPa)	Tensile strength (MPa)	Elongation at break (%)
Copper sheath	130	0.3	395	405	21
Hardened steel inner core	203.4	0.3		Rigid	

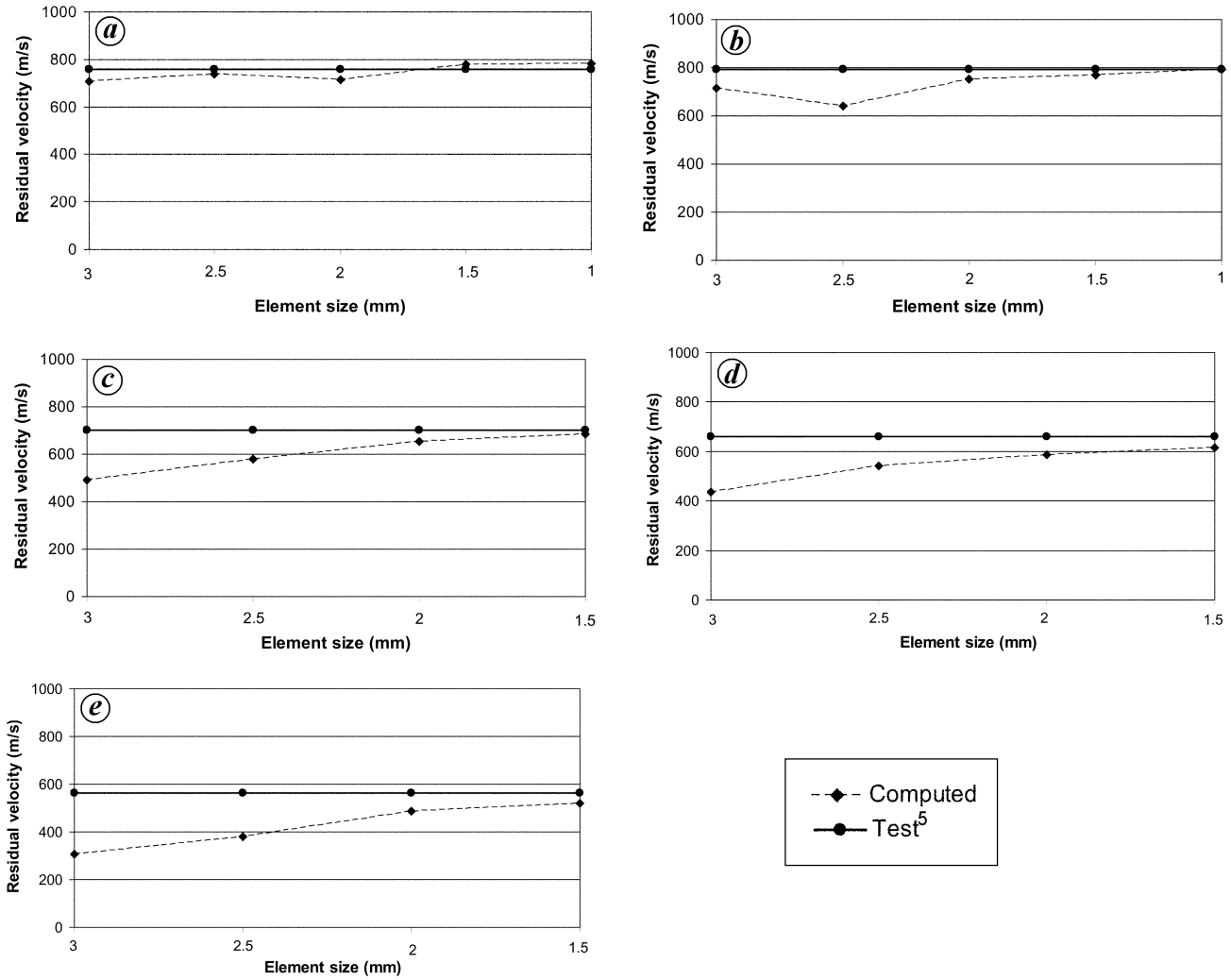

Figure 5. Mesh convergence study for target plates MS1–MS3. ***a***, 4.7 mm thick MS1 plate (projectile impact velocity: 821 m/s); ***b***, 6.0 mm thick MS2 plate (projectile impact velocity: 866.3 m/s); ***c***, 10.0 mm thick MS3 plate (projectile impact velocity: 827.5 m/s); ***d***, 12.0 mm thick MS3 plate (projectile impact velocity: 818 m/s); ***e***, 16.0 mm thick MS3 plate (projectile impact velocity: 819.7 m/s).

and layout of elements, especially in the impact zone, although residual velocity depends primarily on mesh size. The last statement is confirmed in Figure 8, in which in most cases nearly overlapping values of residual velocity are seen for uniform square element-based and circularly symmetric mesh patterns for the target plate.

It may be noted that, in principle, a highly refined uniform square element-based mesh would also give rise to a nearly circular perforation for a target plate impacted by a cylindrical projectile. However, it has been observed by the present authors that excessive mesh refinement leads to deterioration of computed residual velocity compared to the corresponding test residual velocity. This phenomenon may be due to accumulation of rounded-off errors in numerical integration for shell (or even solid) elements caused by an increase in the number of cycles of explicit integration with falling element size. An alternative approach of using a circularly symmetric mesh with triangular elements as shown in Figure 7 (with a reasonable degree of refinement as dictated by convergence requirement) appears to yield a perforation that is visually realistic.

Table 4. Comparison of residual velocity using different types of shell elements in the analysis

Plate material	Plate thickness (mm)	Residual velocity (m/s)	
		Using Belytschko–Lin–Tsay shell elements	Using Hughes–Liu shell elements
MS1	4.7	780.07	780.13
MS2	6.0	748.82	742.14
MS3	10.0	685.93	685.30

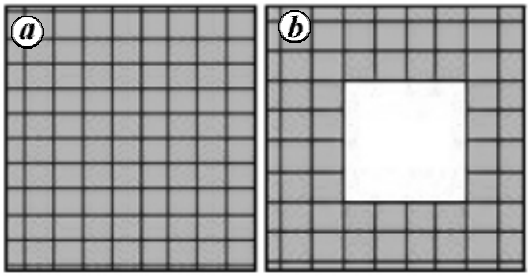

Figure 6. Perforation caused by an ogival-nose projectile on a uniform density mesh with square shell elements (truncated central part of plate target shown). ***a***, Before impact; ***b***, After impact.

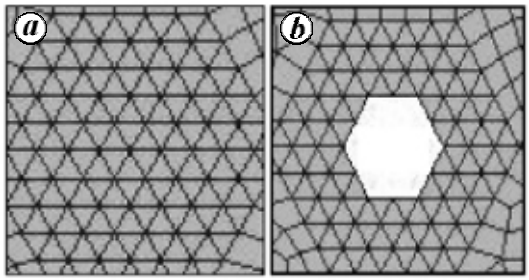

Figure 7. Perforation caused by an ogival-nose projectile on a circularly symmetric mesh in the impact zone (truncated central part of plate target shown). ***a***, Before impact; ***b***, After impact.

Simulation-based failure mechanisms

The ability of the present numerical procedure for predicting residual velocity has been already established. Snap-shots of penetration and perforation of plates MS1–MS3 obtained via analysis are shown in Figure 9. The copper sheath of the projectile is partially eroded during target plate perforation, the extent of which increases with rising plate thickness (Figure 9). Such partial to complete erosion of projectile sheath has been observed earlier[5]. Use of solid elements for representing target plate may further improve the prediction of projectile damage mechanisms. Close-up side and isometric views of the impacted central portion of plate MS1 are shown in Figure 10. Bulging of the plate at the impact location with minimal dishing (i.e. plate bending) is observed in Figure 10 and is consistent with experimental findings at impact velocities above ballistic limit.

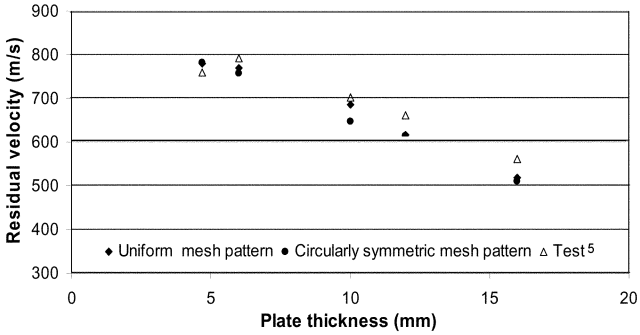

Figure 8. Effect of mesh configuration on residual velocity.

Effect of projectile sheath on residual velocity

It has been opined[4] that projectiles would be more effective in perforation without sheath if extremely high-strength materials are used for the core. This observation is confirmed in Figure 11, in which the analysis has been repeated for three cases (i.e. for 10, 12 and 16 mm thick plates) by removing the copper sheath and retaining the rigid core of the projectile. Figure 11 shows that the assumption of a rigid core (as a limiting case) has led to higher projectile residual velocities; a similar trend can be expected if actual material properties were assigned to an extremely hard-core projectile, so that it will lose less energy during perforation. This would not be the case if an eroding sheath was present.

Effect of strain rate-dependent material modelling of target on residual velocity

One of the key features in the present finite element modelling study is the incorporation of strain-rate effects in the material parameters of the target plate. Ignoring the effects of strain rate would lead to higher projectile residual velocities, as shown in Figure 12. This is expected as quasi-static yield and ultimate strength of the target plate are lower than those at high strain rates.

Numerical parametric studies

Using the geometric and material modelling procedure developed earlier, numerical parametric studies were

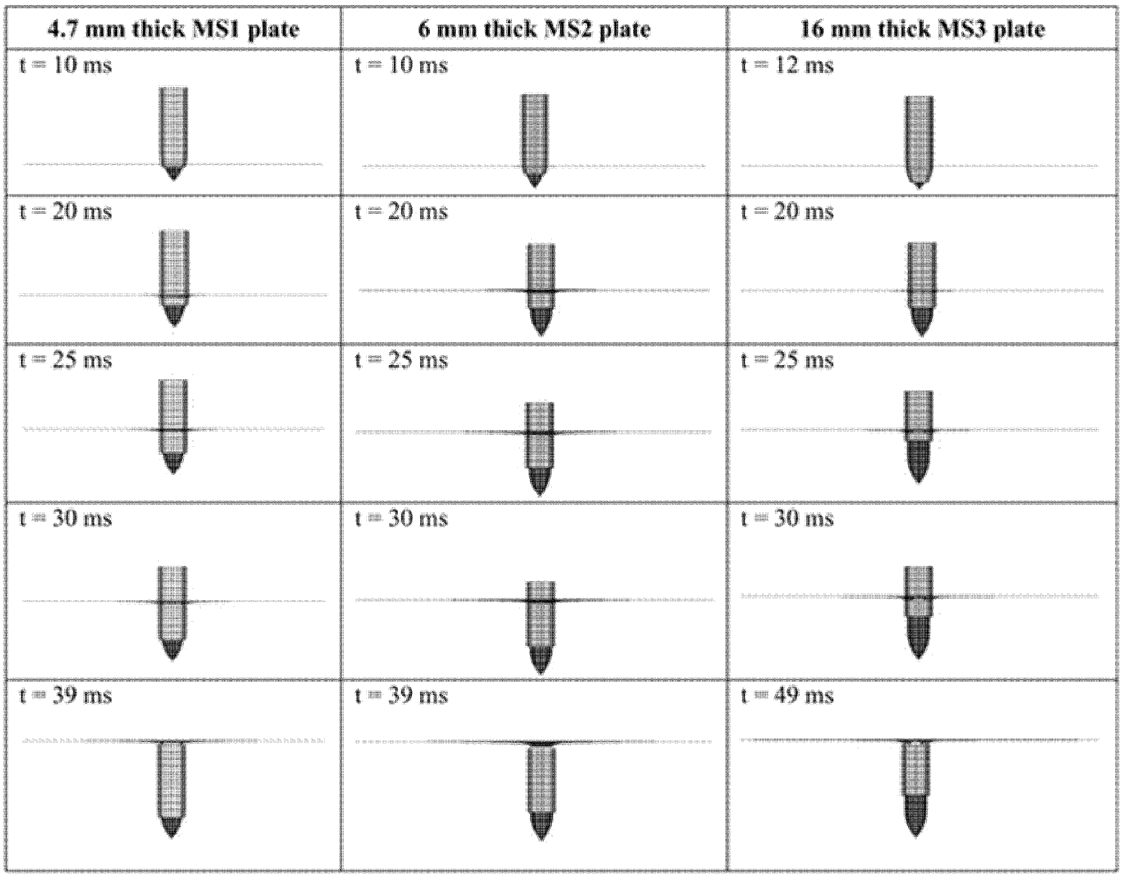

Figure 9. Snap-shots of projectile impact simulation of target plates MS1–MS3.

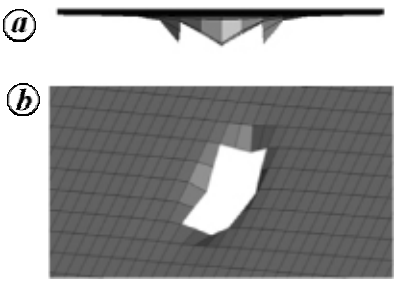

Figure 10. Close-up view of plate bulging and perforation during normal impact on plate MS1. ***a***, Side view; ***b***, Isometric view.

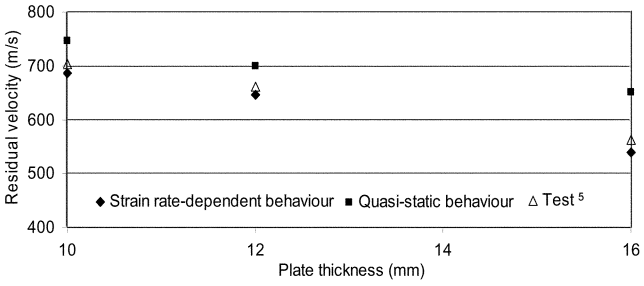

Figure 12. Effect of ignoring material strain rate sensitivity on residual velocity.

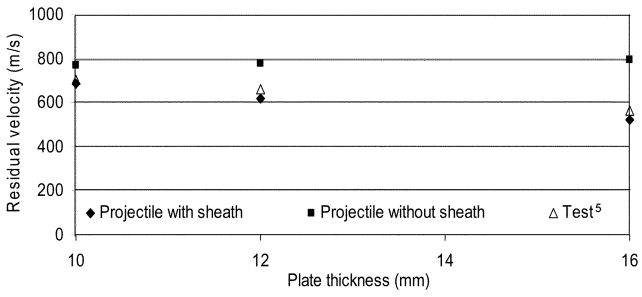

Figure 11. Effect of absence of projectile sheath on residual velocity.

carried out to demonstrate the usefulness of the present simulation methodology as a tool for designing penetration-resistant armour plates. To this end, the effects of plate thickness and projectile diameter on plate performance were considered.

Effect of plate thickness on residual velocity

In order to carry out a rational study on the effect of plate thickness on residual velocity, all projectile and plate para-

meters except plate thickness should be maintained constant. Single-layered plates[5] of five different thicknesses, viz. 4.7, 6, 10, 12 and 16 mm previously analysed were considered. However unlike in Gupta and Madhu[5], where 4.7 and 6 mm plates were of grade MS1 and MS2 respectively, while the remaining plates were of grade MS3, in the present case, plates of all five gauges were at a time assigned the same grade MS1, MS2 or MS3. Thus, a total of ten additional cases had to be analysed and the results are given in Figure 13. For each series of plates of a given material type (i.e. MS1, MS2 or MS3), the best-fit curve for residual velocity versus plate thickness has also been drawn. It is worthwhile to note from Figure 13 that plate MS1, being weaker than plates MS2 and MS3, yielded highest residual velocities, while plate MS2 performed the best, especially at higher thickness due to somewhat superior yield and tensile properties compared to MS3. The patterns of numerically obtained residual velocity variations with plate thickness were similar to the experimental behaviour reported earlier[5].

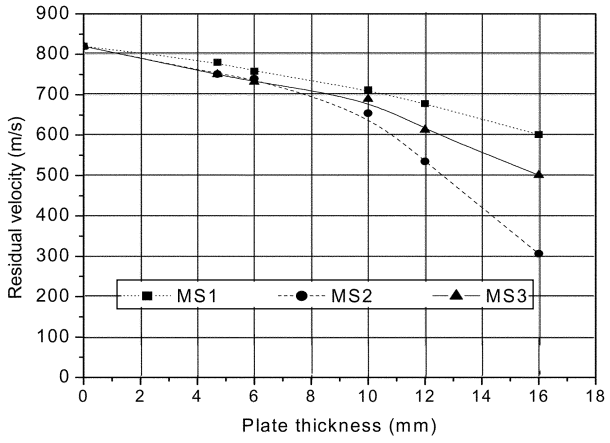

Figure 13. Effect of target plate thickness on projectile residual velocity.

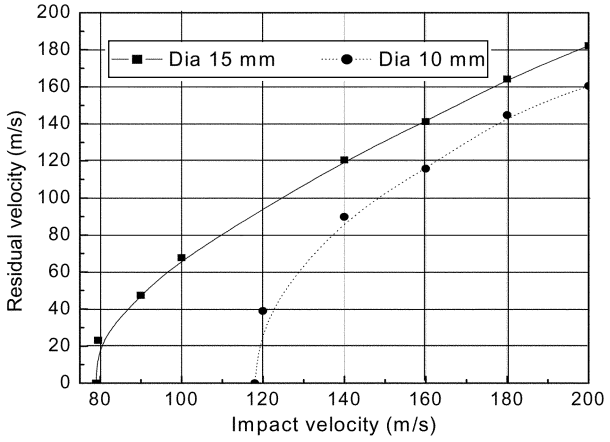

Figure 14. Variations of residual velocity with impact velocity for a given projectile diameter.

Effect of projectile diameter (with constant l/d ratio) on residual velocity

The purpose of this study was to verify whether present finite element-based analyses will qualitatively yield experimentally observed variations[5] of residual velocity with respect to impact velocity for projectiles of different diameters while maintaining the ratio of shank length to diameter (i.e. l/d ratio) as constant. The computed responses for 4.7 mm MS1 plate impacted normally by ogival-nose projectiles of diameter 10 and 15 mm and of a constant l/d ratio of 3.6 are given in Figure 14. Adequate test data are not available for making a direct comparison with the residual velocity curves shown in Figure 14. However, their shapes are typically similar to the test-based variations given by Gupta *et al.*[13] and other researchers for a variety of steel and aluminium target plates. It is especially of interest to note that it would not have been possible to predict the steep drop in residual velocity close to ballistic limit (x-intercept for a given curve in Figure 14) as seen in physical ballistic impact tests, unless the present finite element modelling approach was consistent and robust. It is pointed out that the ballistic limits in Figure 14 have been obtained by following a trial-and-error approach, where ballistic limit is interpreted as the maximum impact velocity at which projectile residual velocity for a target plate just becomes zero.

Conclusions

The present article has dealt with the development of a reliable finite element modelling procedure for predicting residual velocities of projectiles during ballistic impact on MS plates in the ordnance range. A methodical approach has been outlined for material modelling of target plates by accounting for strain rate effects using a standard constitutive model in LS-DYNA. To the best of our knowledge, such a detailed and verifiable study on convergence of residual velocity relative to element size has not been reported in the open literature. A similar comprehensive study needs to be carried out by considering thermal effects which are not likely to be high for the impact velocities in the ordnance range considered here for MS with a melting point that can exceed 1500°C. In the present study, moderately thick target plates were represented with shell elements, and projectiles with solid elements; hence quite arbitrary impact conditions in terms of target geometry as well as impact location and configuration can be simulated. However, previously reported studies were mainly restricted to modelling the impact phenomena with plane strain or axisymmetric elements which would only be applicable to the special case of cylindrical projectiles centrally impacting circular plates. The failure patterns of target plates obtained through simulation were consistent with experimentally

observed failures of steel plates under similar impact conditions. Over-prediction of residual velocity that can result from using quasi-static plate material properties only (by ignoring strain rate sensitivity) has been shown. Furthermore, the advantage of using a rigid projectile without sheath has been demonstrated. Finally, the potential of the current approach as a design tool has been established with the help of numerical parametric studies and obtaining trends consistent with test results reported by previous investigators.

1. Kad, B. K., Schoenfeld, S. E. and Burkins, M. S., Through thickness dynamic impact response in textured Ti-6Al-4V plates. *Mater. Sci. Eng. A*, 2002, **322**, 241–251.
2. Tabiei, A. and Ivanov, I., Computational micro-mechanical model of flexible woven fabric for finite element impact simulation. *Int. J. Num. Methods Eng.*, 2002, **53**, 1259–1276.
3. Espinosa, H. D., Dwivedi, S., Zavattieri, P. D. and Yuan, G., A numerical investigation of penetration in multilayered material/structure systems. *Int. J. Solids Struct.*, 1998, **35**, 2975–3001.
4. Backman, M. E. and Goldsmith, W., The mechanics of penetration of projectile into targets. *Int. J. Eng. Sci.*, 1978, **16**, 1–99.
5. Gupta, N. K. and Madhu, V., An experimental study of normal and oblique impact of hard-core projectile on single and layered plates. *Int. J. Impact. Eng.*, 1992, **19**, 395–414.
6. Benda, Y., Fatigue behaviour of advanced high strength steels for automotive applications. American Iron and Steel, Ispat Inland Inc., February 2003; http://www.autosteel.org
7. Fawaz, Z., Zheng, W. and Behdinan, K., Numerical simulation of normal and oblique ballistic impact on ceramic composite armours. *Compos. Struct.*, 2004, **63**, 387–395.
8. Nandlal, D., Williams, K. and Reza Vaziri, Numerical simulation of the ballistic response of GRP plates. *Compos. Sci. Technol.*, 1998, **58**, 1463–1469.
9. Lim, C. T., Shim, V. P. W. and Ng, Y. H., Finite-element modeling of the ballistic impact of fabric armor. *Int. J. Impact Eng.*, 2003, **28**, 13–31.
10. Shim, V. P. W., Lim, C. T. and Foo, K. J., Dynamic mechanical properties of fabric armour. *Int. J. Impact Eng.*, 2001, **25**, 1–15.
11. Skrzypek, J. J., *Plasticity and Creep* (*Theory, Examples, and Problems*) (English edn, ed. Hetnarski, R. B.), CRC Press, 1993.
12. *LS-DYNA Keyword User's Manual, Version 970*, Livermore Software Technology Corporation, California, 2003.
13. Gupta, N. K., Ansari, R. and Gupta, S. K., Normal impact of ogival nosed projectiles on thin plates. *Int. J. Impact. Eng.*, 2001, **25**, 641–660.

ACKNOWLEDGEMENTS. We thank Prof. J. Srinivasan, IISc, Bangalore for his advice and encouragement. We also thank the reviewers for their helpful suggestions and Prof. K. S. Gandhi for his valuable editorial comments.

Received 21 November 2006; revised accepted 11 April 2007